Volume 50 | Number 6 | 21 January 2014 | Pages 629–752

ChemComm

Chemical Communications

www.rsc.org/chemcomm

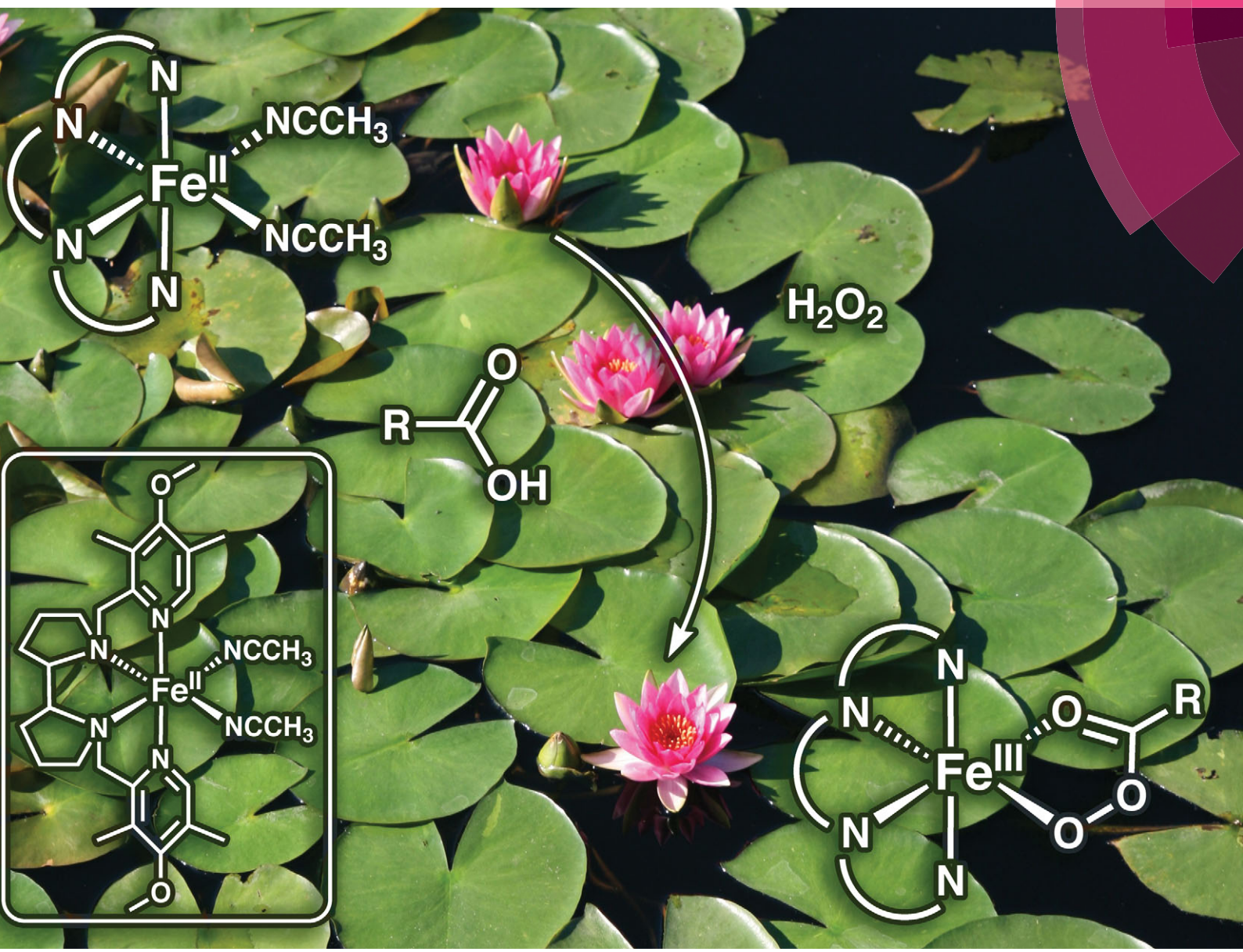

ISSN 1359-7345

ROYAL SOCIETY OF CHEMISTRY

COMMUNICATION

Lawrence Que, Elena V. Rybak-Akimova *et al.*

H_2O_2 activation with biomimetic non-haem iron complexes and AcOH: connecting the g = 2.7 EPR signal with a visible chromophore

ChemComm

COMMUNICATION

View Article Online
View Journal | View Issue

H_2O_2 activation with biomimetic non-haem iron complexes and AcOH: connecting the g = 2.7 EPR signal with a visible chromophore†

Cite this: *Chem. Commun.*, 2014, 50, 645

Received 4th October 2013,
Accepted 11th November 2013

DOI: 10.1039/c3cc47632d

www.rsc.org/chemcomm

Olga V. Makhlynets,[a] Williamson N. Oloo,[b] Yurii S. Moroz,[a] Irina G. Belaya,[a] Taryn D. Palluccio,[a] Alexander S. Filatov,[c] Peter Müller,[d] Matthew A. Cranswick,[b] Lawrence Que, Jr.*[b] and Elena V. Rybak-Akimova*[a]

Mechanistic studies of H_2O_2 activation by complexes related to $[(BPMEN)Fe^{II}(CH_3CN)_2]^{2+}$ with electron-rich pyridines revealed that a new intermediate formed in the presence of acetic acid with a 465 nm visible band can be associated with an unusual g = 2.7 EPR signal. We postulate that this chromophore is an acylperoxoiron(III) intermediate.

$[Fe^{II}(BPMEN)(CH_3CN)_2]^{2+}$ (**1a**, Scheme 1) is a prototypical model for non-haem iron enzymes, which activates H_2O_2 to catalyse olefin epoxidation and alkane hydroxylation with high stereoselectivity,[1,2] and catalyst performance can be improved by the addition of acetic acid.[3,4] Subsequently, it was demonstrated that replacing the 1,2-diaminoethane backbone of **1a** with 2,2′-bipyrrolidine to produce **1b** improved the regioselectivity of aliphatic hydroxylation in natural products.[5] A mechanism for H_2O_2 activation by non-haem iron complexes with aminopyridine ligands was proposed by Que[1–3,6] on the basis of extensive work with closely related $[Fe^{II}(TPA)(CH_3CN)_2]^{2+}$ (**1e**, Scheme 1). **1e** reacts with H_2O_2 to produce well-characterized $Fe^{III}(OOH)$[2,7,8] and $Fe^{IV}{=}O$[3] intermediates, neither of which is kinetically competent for olefin epoxidation.[3,6] Parallel experiments with **1a** have shown that the corresponding $Fe^{III}(OOH)$ species does not hydroxylate benzene directly and acetic acid accelerates the formation of a metal-based oxidant responsible for aromatic hydroxylation.[9] For both **1a** and **1e**, a yet to be observed $Fe^{V}{=}O$ was proposed to be the oxidizing species, which may form by O–O bond heterolysis of $Fe^{III}(OOH)$ promoted by the coordinated acetic acid.[3] In this work, we introduced electron donating substituents onto the pyridine donors of **1a** and **1b** to make corresponding **1c** and **1d** (Scheme 1) with the goal of stabilizing higher-valent intermediates in the catalytic cycles of these complexes, an approach previously demonstrated in diiron(IV) chemistry.[10] Herein we describe new intermediates generated from **1c**/**1d**, H_2O_2, and RCOOH.

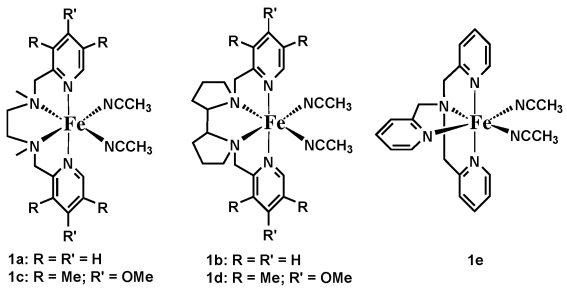

Scheme 1 Structures of Fe^{II} complexes used in this work.

Complexes **1c** and **1d**[11] were readily synthesized following procedures for **1a** and **1b** with some modifications (see ESI† for details, Fig. S1–S3). Their X-ray structures reveal distorted octahedral iron(II) centers (Fig. S4, ESI†) with both tetradentate ligands adopting a *cis*-α-topology and show average Fe–N bond lengths of 2.0 Å typical for low-spin aminopyridine iron(II) complexes. The *cis* orientation of the labile CH_3CN ligands is important for H_2O_2 activation during catalysis.[12] As expected, **1c** and **1d** exhibited $Fe^{III/II}$ reduction potentials *ca.* 130 mV lower than their unsubstituted counterparts (Table S1 and Fig. S5–S8, ESI†); they also undergo oxidation even with trace O_2 to form diferric complexes (Fig. S9, ESI†).

We have previously shown that **1a** reacts with H_2O_2 to give a short-lived $Fe^{III}(OOH)$ intermediate (**2a**).[9] Unlike other non-haem $Fe^{III}(OOH)$ intermediates, which can be generated in higher yields at lower temperature, no $Fe^{III}(OOH)$ was observed when **1a** and H_2O_2 were mixed at or below −30 °C, but the yield of $Fe^{III}(OOH)$ increased as the temperature was raised to 20 °C.[6,9] **1b**, **1c**, and **1d** also reacted with H_2O_2 to afford $Fe^{III}(OOH)$ intermediates with λ_{max} = 550–560 nm (Fig. 1 and Fig. S10 and S11, ESI†). With the latter complexes, however, the rates of $Fe^{III}(OOH)$ formation were notably faster (Table S1, ESI†) and significantly exceeded their rates of decay

[a] *Department of Chemistry, Tufts University, 62 Talbot Avenue, Medford, Massachusetts 02155, USA. E-mail: erybakak@tufts.edu; Fax: +1-6176273443; Tel: +1-6176273413*
[b] *Department of Chemistry and Center for Metals in Biocatalysis, University of Minnesota, 207 Pleasant Street S.E., Minneapolis, USA*
[c] *Department of Chemistry, University at Albany, 1400 Washington Avenue, Albany, New York 12222, USA*
[d] *Department of Chemistry, Massachusetts Institute of Technology, 77 Massachusetts Ave, Cambridge, USA*

† Electronic supplementary information (ESI) available: synthesis and characterization of ligands and complexes, details of EPR, stopped-flow, CV, and GCMS experiments. CCDC 964529–964531 and 964853. For ESI and crystallographic data in CIF or other electronic format see DOI: 10.1039/c3cc47632d

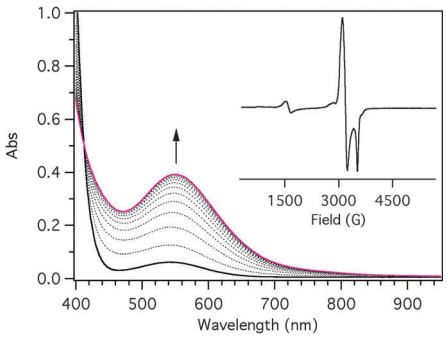

Fig. 1 UV-Vis spectra for **2d** formation upon mixing **1d** (1 mM) with H_2O_2 (10 mM) at 20 °C in CH_3CN, with maximum accumulation seen at 2 s after mixing reagents (shown in the graph). Inset: EPR spectrum (2.4 K) of **2d** frozen immediately upon mixing **1d** (1 mM) and H_2O_2 (10 mM) in CH_3CN at 10 °C; *g* values are at 2.22, 2.16 and 1.96.

to allow these species to be trapped and characterized at −30 °C (Fig. S12, ESI†). Intermediates **2b**, **2c** and **2d** all exhibited EPR signals with *g*-values at *ca.* 2.22, 2.16, and 1.96, similar to those reported for other low-spin Fe^{III}(OOH) complexes[13] (Fig. 1, Fig. S13 and S14, Table S2, ESI†). Spin quantification of the EPR signal of **2d** shown in Fig. S15 (ESI†) revealed that it represents ~36% of the Fe in that sample.

Addition of acetic acid to Fe^{II}(L)–H_2O_2 catalytic mixtures has been shown to enhance substrate oxidation. To gain insight into how the Fe^{III}(OOH) intermediate may be altered, we have investigated the reaction between **2d** and AcOH by stopped-flow spectrophotometry. When AcOH was added upon maximum formation of **2d**, a new intermediate with λ_{max} = 465 nm (**3d**) accumulated quickly (1 s at 20 °C, Fig. 2). Species **3d** was unstable and decayed into a species **4d** with λ_{max} = 740 nm that can be assigned to a low spin Fe^{IV}=O complex based on the position of its near IR band (Fig. 2, Scheme 2);[14] **4d** can also be independently generated by reaction of **1d** and IBX-ester (Fig. S16, ESI†). Similarly, **2c** converts to **3c** upon addition of AcOH, which in turn decayed into **4c** (Fig. S17, ESI†).

Intermediate **3d** can also be generated in one step by mixing **1d**, H_2O_2 and AcOH (Fig. 2, inset) and ultimately decayed into a

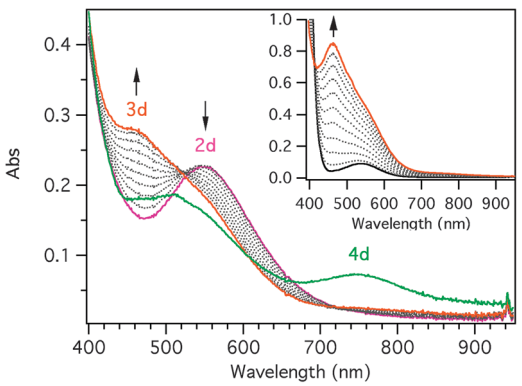

Fig. 2 Spectral changes upon addition of AcOH to Fe^{III}(OOH) in CH_3CN at 20 °C. **2d** (purple line) was generated from **1d** (0.5 mM) and H_2O_2 (5 mM) in the first mixing (aging time 2 s); AcOH (0.5 mM) was then added in the second mixing to form **3d** within 1 s (orange line). **3d** decayed over 47 s at 20 °C into a species **4d** with λ_{max} = 740 nm (green line). Inset: **1d** (1 mM, *t* = 0, black line) reacts with a mixture AcOH–H_2O_2 (1 mM/5 mM) at −30 °C to produce **3d** (*t* = 62 s, orange line).

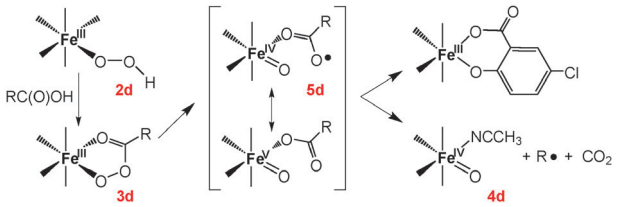

Scheme 2 Formation of **3d** and its subsequent self-hydroxylation.

species with λ_{max} = 740 nm (**4d**). Interestingly the yield of **3d** did not depend significantly on H_2O_2 concentration when AcOH was limiting (1 equiv. *vs.* **1d**), suggesting that AcOH was incorporated into the chromophore of **3d** (Fig. S18, ESI†). A likely scenario is the reaction of acetic acid with the bound hydroperoxide to form an acylperoxo ligand at the iron center, a process that may be promoted by the non-haem iron center.[15]

To test this hypothesis, **1d** was reacted with peroxyacids. As peroxyacetic acid was available only in a mixture with acetic acid (which accelerates the formation of an unreactive (μ-oxo)(μ-carboxylato)diiron(III) side-product[16]), $AdCO_3H$[17] was used as an alternative peroxyacid obtainable in pure form. Indeed, reaction of **1d** with both $AdCO_3H$ and H_2O_2–AdCOOH in acetonitrile at −30 °C afforded the 465 nm chromophore associated with **3d** (Fig. S19, ESI†). Similarly, **3d** was observed to form when **1d** was mixed with *m*-chloroperoxybenzoic acid (*m*CPBA), but this case was complicated by the subsequent appearance of a blue chromophore associated with an Fe^{III}-salicylate product resulting from self-hydroxylation (Fig. S20, ESI†).[18–20]

To further characterize the 465 nm chromophore, we obtained EPR spectra of samples generated by mixing **1d** and AcOH–H_2O_2 or *m*CPBA and frozen upon maximum accumulation of the 465 nm chromophore. These spectra showed a mixture of *S* = 1/2 species (Fig. 3, Fig. S21 and S22, ESI†) not observed in the EPR spectrum of **2d** (Fig. 1). This suggests that the conversion of **2d** to **3d** is not a straightforward transformation, consistent with the lack of a true isosbestic point in the UV-Vis data in Fig. 2. The *g* = 2.72 and 2.42 signals of **3d** were well resolved from other *S* = 1/2 signals in Fig. 3; their integration relative to an external copper signal corresponds to ~7% of the iron in the sample. Similar signals were previously observed by Talsi[21,22] and Richens[23] in the reactions of various non-haem Fe^{II}(N4) complexes (N4 = TPA, L_a, or L_b) with AcOH–H_2O_2 or

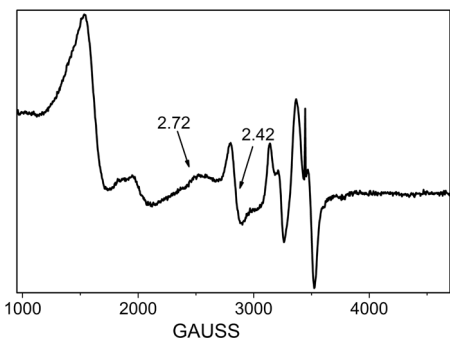

Fig. 3 EPR spectrum acquired at 10 K of an aliquot frozen upon maximum formation of **3d** in the reaction of **1d** (1 mM) with H_2O_2 (10 equiv.) and AcOH (2 equiv.) in CH_3CN at −30 °C.

*m*CPBA (Table S3, ESI†), but no UV-Vis data were reported. Thus the fact that we can observe the g = 2.7 signal only when the 465 nm chromophore was present allows us *for the first time* to connect these spectroscopic features with each other.

The g = 2.7 signal has been assigned by Talsi to a novel $[(N4)Fe^{V}{=}O(X)]^{2+}$ species that carried out substrate oxidation.[21,22] On the other hand, Richens proposed instead a low-spin $[(TPA)Fe^{III}(O_3CC_6H_4\text{-}3\text{-}Cl)]^{2+}$ complex,[23] due to the resemblance of the EPR features to those observed for highly anisotropic low-spin ferric centers found in haem complexes.[24] In support of the latter formulation, acylperoxoiron(III) complexes have been reported by Suzuki, Furutachi *et al.* to have visible chromophores similar to that of **3d**,[25,26] and one of these, $[Fe^{III}(6Me_2\text{-}BPP)(\kappa^2\text{-}OOC(O)Me)]^{2+}$ ($6Me_2$-BPP = bis(6-methyl-2-pyridylmethyl)-3-aminopropionate), has even been crystallographically characterized. A transient S = 1/2 species with a purple color (λ_{max} = 535 nm) has also been found by Mirica *et al.* in the reaction of peracetic acid with $[Fe^{II}(^{tBu}N4)(NCMe)_2]^{2+}$ ($^{tBu}N4$ = *N*,*N*′-di-*tert*-butyl-2,11-diaza[3.3](2,6)pyridinophane),[27] which may arise from an acylperoxoiron(III) complex. Based on the above points, we also favour the assignment of **3d** as a low-spin acylperoxoiron(III) species. Clearly we need to increase its concentration to perform more detailed spectroscopic analysis that can establish the oxidation state of its iron center.

As noted above, **3d** was also formed in the reaction of **1d** with *m*CPBA prior to the appearance of the blue Fe^{III}-salicylate product (Fig. S20, ESI†), implicating the role of **3d** as a precursor. This observation is related to a previous report that AcOH accelerated the **1a**-promoted hydroxylation of benzene with H_2O_2 as an oxidant.[9] Likewise **1b–1d** promote aromatic hydroxylation using H_2O_2 as evidenced by the formation of blue Fe^{III}–phenolate or Fe^{III}–salicylate complexes, as also reported by Banse *et al.* for a related $Fe^{II}(N5)$ complex.[28] The role of **3d** in aromatic hydroxylation was thus explored by double-mixing stopped-flow studies, wherein **3d** was initially generated by the combination of **1d**, 1–4 equiv. H_2O_2, and 1 equiv. AcOH and then reacted with 2 equiv. benzoic acid. A band with $\lambda_{max} \sim 600$ nm was observed, corresponding to formation of an Fe^{III}–salicylate product, indicating that **3d** or a species derived from it can effect aromatic hydroxylation (Fig. S23, ESI†). On the other hand, when benzene (300 equiv.) was used instead of benzoic acid, phenol product formation was not observed with 1 equiv. of H_2O_2, although hydroxylation occurred with excess H_2O_2 (Fig. S24, ESI†). A likely rationale for this reactivity difference is the binding of benzoate to the iron center, which provides an entropic advantage inherent in an intramolecular reaction.

Assuming that **3d** is the acylperoxoiron(III) species, we propose that hydroxylation of the R group on the acylperoxo ligand can only occur subsequent to O–O bond cleavage in order for the terminal acylperoxo O-atom to be in a position to attack the R group (Scheme 2). Recent DFT calculations[29] on the reaction of **1b** and H_2O_2–AcOH revealed that an acylperoxoiron(III) species formed as a stable intermediate that subsequently underwent O–O bond cleavage to carry out substrate oxidation. Thus a yet unobserved $Fe^{V}(O)(O_2C\text{–}Ar)$ species or its $Fe^{IV}(O)(^{\bullet}O_2C\text{–}Ar)$ electromer (**5d**) would likely act as the actual oxidant in such reactions. With a visible spectroscopic handle at 465 nm now available for **3d**, more extensive kinetic studies are underway to gain insight into how **3d** reacts with substrates.

In summary, we have reported the structural characterization of two new ferrous complexes **1c** and **1d**, which are analogs of **1a** and **1b** with electron-donating substituents on the pyridine donors. **1c** and **1d** react with either H_2O_2–AcOH or peroxyacids to afford intermediates **3c** and **3d** with a new visible chromophore at λ_{max} = 465 nm. S = 1/2 EPR signals at g = 2.7 and 2.4 are observed for intermediate **3d** (Fig. 3), which are distinct from those associated with the $(L)Fe^{III}(OOH)$ complexes **2c** and **2d** (g = 2.22, 2.16, and 1.96, inset of Fig. 1) that are formed by reaction with H_2O_2 alone. In the absence of a substrate, intermediates **3** decay into the corresponding $Fe^{IV}(O)$ complexes **4**. We propose **3c** and **3d** to be $(L)Fe^{III}(O_3C\text{–}R)$ species that undergo O–O bond cleavage to afford a yet unobserved higher-valent oxidant responsible for subsequent oxidative transformations (*e.g.* aromatic hydroxylation). The intermediacy of $Fe^{III}(O_3C\text{–}R)$ *vs.* $Fe^{III}(OOH)$ rationalizes reactivity differences in iron-catalyzed oxidations with H_2O_2 with and without carboxylic acids.

This work was funded by DOE grant DE-FG02-06ER15799 to E.V.R.-A. and grant DE-FG02-03ER15455 to L.Q. Kinetic and crystallographic instrumentation was supported by the NSF.

Notes and references

1 K. Chen and L. Que, Jr., *J. Am. Chem. Soc.*, 2001, **123**, 6327–6337.
2 K. Chen, M. Costas, J. Kim, A. K. Tipton and L. Que, Jr., *J. Am. Chem. Soc.*, 2002, **124**, 3026–3035.
3 R. Mas-Ballesté and L. Que, Jr., *J. Am. Chem. Soc.*, 2007, **129**, 15964–15972.
4 M. C. White, A. G. Doyle and E. N. Jacobsen, *J. Am. Chem. Soc.*, 2001, **123**, 7194–7195.
5 M. S. Chen and M. C. White, *Science*, 2007, **318**, 783–786.
6 W. Oloo, A. J. Fielding and L. Que, Jr., *J. Am. Chem. Soc.*, 2013, **135**, 6438–6441.
7 C. Kim, K. Chen, J. Kim and L. Que, Jr., *J. Am. Chem. Soc.*, 1997, **119**, 5964–5965.
8 A. Mairata i Payeras, R. Y. N. Ho, M. Fujita and L. Que, Jr., *Chem.–Eur. J.*, 2004, **10**, 4944–4953.
9 O. V. Makhlynets and E. V. Rybak-Akimova, *Chem.–Eur. J.*, 2010, **16**, 13995–14006.
10 G. Xue, R. De Hont, E. Münck and L. Que Jr., *Nat. Chem.*, 2010, **2**, 400–405.
11 O. Cussó, I. Garcia-Bosch, X. Ribas, J. Lloret-Fillol and M. Costas, *J. Am. Chem. Soc.*, 2013, **135**, 14871–14878.
12 L. Que, Jr. and W. B. Tolman, *Nature*, 2008, **455**, 333–340.
13 M. Costas, M. P. Mehn, M. P. Jensen and L. Que, Jr., *Chem. Rev.*, 2004, **104**, 939–986.
14 A. R. McDonald and L. Que, Jr., *Coord. Chem. Rev.*, 2013, **257**, 414.
15 M. Fujita and L. Que, Jr., *Adv. Synth. Catal.*, 2004, **346**, 190–194.
16 S. Taktak, S. V. Kryatov, T. E. Haas and E. V. Rybak-Akimova, *J. Mol. Catal. A: Chem.*, 2006, **259**, 24–34.
17 L. S. Silbert, E. Siegel and D. Swern, *J. Org. Chem.*, 1962, **27**, 1336–1342.
18 O. V. Makhlynets, P. Das, S. Taktak, M. Flook, R. Mas-Ballesté, E. V. Rybak-Akimova and L. Que, Jr., *Chem.–Eur. J.*, 2009, **15**, 13171–13180.
19 N. Y. Oh, M. S. Seo, M. H. Lim, M. B. Consugar, M. J. Park, J.-U. Rohde, J. Han, K. M. Kim, J. Kim, L. Que, Jr. and W. Nam, *Chem. Commun.*, 2005, **45**, 5644–5646.
20 S. Taktak, M. Flook, B. M. Foxman, L. Que, Jr. and E. V. Rybak-Akimova, *Chem. Commun.*, 2005, **42**, 5301–5303.
21 O. Y. Lyakin, K. P. Bryliakov, G. J. P. Britovsek and E. P. Talsi, *J. Am. Chem. Soc.*, 2009, **131**, 10798–10799.

22 O. Y. Lyakin, R. V. Ottenbacher, K. P. Bryliakov and E. P. Talsi, *ACS Catal.*, 2012, **2**, 1196–1202.
23 G. Guisado-Barrios, Y. Zhang, A. M. Harkins and D. T. Richens, *Inorg. Chem. Commun.*, 2012, **20**, 81–85.
24 D. Inniss, S. M. Soltis and C. E. Strouse, *J. Am. Chem. Soc.*, 1988, **110**, 5644–5650.
25 K. Hashimoto, S. Nagamoto, S. Fujinami, H. Furutachi, S. Ogo, M. Suzuki, A. Uehara, Y. Maeda, Y. Watanabe and T. Kitagawa, *Angew. Chem., Int. Ed.*, 2002, **41**, 1202–1205.
26 X. Zhang, H. Furutachi, T. Tojo, T. Tsugawa, S. Fujinami, T. Sakurai and M. Suzuki, *Chem. Lett.*, 2011, **40**, 515–517.
27 J. R. Khusnutdinova, J. Luo, N. P. Rath and L. M. Mirica, *Inorg. Chem.*, 2013, **52**, 3920–3932.
28 A. Thibon, V. Jollet, C. Ribal, K. Sénéchal-David, L. Billon, A. B. Sorokin and F. Banse, *Chem.–Eur. J.*, 2012, **18**, 2715–2724.
29 Y. Wang, D. Janardanan, D. Usharani, K. Han, L. Que, Jr. and S. Shaik, *ACS Catal.*, 2013, **3**, 1334–1341.

